JOURNAL OF CATALYSIS 104, 1–16 (1987)

Calorimetric Heat of Adsorption Measurements on Palladium

I. Influence of Crystallite Size and Support on Hydrogen Adsorption

PEN CHOU AND M. ALBERT VANNICE

Department of Chemical Engineering, The Pennsylvania State University, University Park, Pennsylvania 16802

Received July 9, 1986; revised September 30, 1986

A modified differential scanning calorimeter was used to measure integral heats of adsorption of hydrogen, Q_{ad}, at 300 K on unsupported Pd powder and on Pd dispersed on SiO_2, SiO_2–Al_2O_3, Al_2O_3, and TiO_2. The supports were found to have no significant effect on Q_{ad}, and although reduction of Pd/TiO_2 samples at 773 K sharply decreased the amount of hydrogen chemisorbed on these samples, the Q_{ad} values measured on these samples were comparable to the other catalysts. In contrast, Pd crystallite size had a very pronounced effect on Q_{ad}. On all these catalysts the heat of adsorption for hydrogen remained constant at 15 ± 1 kcal mole^{-1} as the average Pd crystallite size decreased from 1000 to 3 nm, but it increased sharply as the size dropped below 3 nm. The highest value, 24 kcal mole^{-1}, was obtained on one of the most highly dispersed samples. Heats of formation of bulk Pd hydride showed a similar behavior, remaining constant at 8.7 ± 1.0 kcal mole^{-1} for samples with low Pd dispersions and then increasing noticeably as the crystallite size dropped below 3 nm. Most of this variation in Q_{ad} is attributed to changes in the electronic properties of small Pd crystallites because the differences in Q_{ad} values reported on single crystal surfaces are not sufficient to explain the enhanced bond strength.

INTRODUCTION

Chemisorption is an essential step in heterogeneous catalysis; consequently, the bonding strength between adsorbate and catalyst is an extremely important parameter in surface reactions. The strength of chemisorption bonds can affect not only the activation energy of a surface reaction but also the surface concentration of reactants, and the effects of heats of adsorption on a surface reaction are clearly illustrated in a Langmuir–Hinshelwood type of rate equation. In addition, it is important to realize that heats of adsorption also reflect surface properties of the adsorbent, and an example of the correlation between catalytic activities of different metals and heats of adsorption was given by Beeck in one of his pioneer studies of hydrogenation catalysts (*1*).

It is not surprising that changes in heats of adsorption have often been cited as one of the origins for observed variations in catalytic properties or chemisorption behavior on supported catalysts. Studies have shown that the use of particular supports to disperse a metal component, such as TiO_2, can markedly decrease the chemisorption capacity after a high-temperature reduction (HTR) (*2, 3*). Electron microscopy and X-ray diffraction studies have shown that the large decrease in chemisorption capacity is not due to sintering of the metal particles (*2*). It was originally suggested by Tauster *et al.* that an electronic interaction between the metal atoms and reduced cations on the support may weaken the adsorbate–metal interaction and thereby decrease chemisorption uptakes (*4*). Similar electronic interactions between metal and support have also been proposed as the cause of support effects observed with other supported catalysts. Alternatively, it was first suggested by Naccache and co-workers (*5*) and Santos *et al.* (*6*) that the decrease in chemisorption is due to physical blockage of chemisorption sites by titanium oxide

0021-9517/87 $3.00

species that migrate onto the metal surface during reduction. This process could account for the large decrease in chemisorption capacity without invoking changes in adsorption bond strengths.

The size of metal particles is another factor that is known to affect catalytic properties of metals in structure-sensitive reactions (*7*). Size effects in metal crystallites are often attributed either to a change in electronic properties (*8*) or in surface geometric structure (*9*); however, both vary simultaneously for very small crystallites. As the particle size drops below a certain value, electronic properties of metal crystallites begin to deviate from those of bulk metal and the average coordination number of surface atoms decreases, and both effects may alter the state of bonding between adsorbate and metal.

Although heat of adsorption values have been obtained for Pd single crystals, films, and filaments in ultrahigh-vacuum (UHV) systems, there have been few measurements on supported Pd and no systematic investigation of the influence of crystallite size or the support on this parameter. Consequently, we initiated a study of heats of adsorption on supported catalysts to fill this gap and to determine if the decrease in chemisorption in Pd/TiO_2 catalysts is primarily chemical or physical in nature. Because methods applicable in UHV systems are much more difficult to apply to porous materials, we have used a modified differential scanning calorimeter (DSC) to measure integral, isothermal heats of adsorption (*10*). In this paper we report not only the heats of adsorption of H_2 measured over a wide range of Pd crystallite size using SiO_2, SiO_2–Al_2O_3, Al_2O_3, and TiO_2 as supports but also heats of formation of the Pd β-hydride phase. Similar studies of CO and O_2 adsorption are reported separately (*11, 12*).

EXPERIMENTAL

Catalyst Preparation

The supports used in this study were SiO_2 (Davison Grade 57–220 $m^2\ g^{-1}$), SiO_2–Al_2O_3 (Davison Grade 979—13% alumina, 400 $m^2\ g^{-1}$), η-Al_2O_3 (Exxon Research & Engineering Co., 245 $m^2\ g^{-1}$), and TiO_2 (Degussa P25—80% anatase and 20% rutile, 50 $m^2\ g^{-1}$). All support materials were calcined at 773 K in flowing air for 4 h prior to metal loading. Different Pd precursors were used to prepare catalysts with the methods described as follows.

(*i*) *Wet impregnation* (*WI*). An aqueous solution of H_2PdCl_4 prepared from $PdCl_2$ (Ventron Corp.) and dilute hydrochloric acid was used for most of the catalysts prepared by impregnation. Two catalysts were prepared from palladium acetylacetonate (Aldrich Co.) dissolved in excess benzene (Baker Analyzed) (*13*). The impregnated catalysts were then dried overnight in air at 393 K.

(*ii*) *Ion exchange* (*IE*). Several catalysts were prepared by ion exchange between $Pd(NH_3)_4(NO_3)_2 \cdot 2H_2O$ (Spex) dissolved in deionized, distilled (D,D) water and SiO_2, SiO_2–Al_2O_3, and η-Al_2O_3 at pH = 9, 10, and 11, respectively. A Pd/Al_2O_3 catalyst was also prepared by ion exchange with a H_2PdCl_4 solution at pH = 3. The IE catalysts were washed with D,D water and dried in air at 393 K for 3 h. All the catalysts except for the last one were then calcined at 573 or 773 K in flowing air or in a mixture of 15 $cm^3\ min^{-1}$ O_2 and 60 $cm^3\ min^{-1}$ He for 2 h.

(*iii*) *Unsupported Pd.* An unsupported Pd sample was prepared from Pd powder (Johnson Matthey Chemicals, Puratronic Grade 1—impurities detected: Si, 2 ppm; Fe, 1 ppm; Ca, Cu, and Ag each less than 1 ppm) by cleaning the powder in a flowing mixture of 20% O_2 and 80% He at 773 K for 30 min, then reducing at 573 K in a flowing mixture of 20% H_2 and 80% He for 1 h.

The Pd weight loadings of the supported catalysts were determined by plasma emission spectroscopy and neutron activation analysis, and they are listed with the preparation method in Table 1. Pure support blanks were prepared by impregnating

TABLE 1

Preparation Methods for Pd Catalysts

Catalyst	Precursor	Method[a]	Calcination temperature (K)
1.71% Pd/SiO_2	$PdCl_2$	WI	None
0.48% Pd/SiO_2	$Pd(NH_3)_4(NO_3)_2$	IE	573
2.10% Pd/SiO_2	$Pd(NH_3)_4(NO_3)_2$	IE	573
0.39% Pd/SiO_2	$Pd(NH_3)_4(NO_3)_2$	IE	573
1.23% Pd/SiO_2	$Pd(NH_3)_4(NO_3)_2$	IE	573
1.95% Pd/SiO_2–Al_2O_3	$PdCl_2$	WI	None
1.16% Pd/SiO_2–Al_2O_3	$Pd(NH_3)_4(NO_3)_2$	IE	573
0.98% Pd/SiO_2–Al_2O_3	$Pd(NH_3)_4(NO_3)_2$	IE	573
1.80% Pd/Al_2O_3	$PdCl_2$	WI	None
0.32% Pd/Al_2O_3	$Pd(C_5H_7O_2)_2$	WI	573
0.36% Pd/Al_2O_3	$PdCl_2$	IE	None
0.54% Pd/Al_2O_3	$Pd(NH_3)_4(NO_3)_2$	IE	573
2.33% Pd/Al_2O_3	$PdCl_2$	WI	None
2.03% Pd/TiO_2	$PdCl_2$	WI	None
1.88% Pd/TiO_2	$Pd(C_5H_7O_2)_2$	WI	773
Pd powder	—	—	773

[a] WI, wet impregnation; IE, ion exchange.

calcined support materials with D,D water and then drying overnight in air at 393 K.

Chemisorption

The chemisorption uptakes were measured in a volumetric adsorption system equipped with an Edwards Model E02 oil diffusion pump backed by a GCA Vac-Torr Model 150 mechanical pump and liquid N_2 traps, which produced an ultimate vacuum near 5×10^{-7} Torr. A Texas Instruments precision pressure gauge and a Granville–Phillips Model 260-002 ionization gauge were used to measure the pressures. Further details have been given elsewhere (*14*).

After calcination (if used), ~0.4-g catalyst samples prepared by the impregnation method were heated in 50 cm^3 min^{-1} of He from room temperature to 448, 533, 673, or 723 K prior to a 1-h reduction in 50 cm^3 min^{-1} of H_2 or in a mixture of 15 cm^3 min^{-1} of H_2 and 60 cm^3 min^{-1} of He at 448, 673, 723, or 773 K. The catalysts prepared by ion exchange were treated in 50 cm^3 min^{-1} of He at 573 K for 1 h, cooled to room temperature, and then reduced in a flowing gas mixture of H_2 and He as stated above. All the samples were given one of the above pretreatments and stored in a desiccator before chemisorption measurements.

The method described by Benson *et al.* (*15*) was used to determine chemisorption uptakes of hydrogen at 300 K on each sample. After the first H_2 uptake was measured, the sample was evacuated for 25 min at 300 K and a second isotherm was measured to determine the uptake of H_2 due to bulk hydride formation. Each measurement of H_2 uptake was repeated at least once to ensure that the Pd dispersion had stabilized. Chemisorption of CO on three of the samples (noted in Table 2) was also determined at this stage, and in these cases, the samples were treated in a flowing gas mixture of 20% O_2 and 80% He at 573 K for 30 min after each CO uptake measurement to facilitate complete removal of CO. A portion of each of these samples was then used for heat of adsorption measurements and Pd weight loadings. The portion left was used for additional measurements of H_2, O_2, and CO uptakes after subsequent pretreat-

ments paralleling those in the calorimeter (*11, 12*).

Calorimetric Measurements

Energy changes during chemisorption and bulk Pd hydride formation at 300 K were measured in a modified Perkin–Elmer DSC-2C differential scanning calorimeter. The calorimeter has two identical sample holders located inside two cavities in an aluminum block which were constantly purged with gas from a gas handling system. The gas handling system consisted mainly of gas purifiers, mass flow controllers, and a switching valve to allow switching between a portion of the purge gas (He or Ar) and the adsorbate (H_2, O_2, or CO). Ultrahigh purity argon (99.999%, MG Scientific Gases) was further purified by passing it first through a drying tube (Supelco Inc.), and then through an Oxytrap (Alltech Associates). The helium (99.999%, MG Scientific) was purified in a similar fashion. Ultrapure hydrogen (<10 ppb total impurities) was produced electrolytically in an Elhygen Mark V hydrogen generator and purified by diffusing the hydrogen through a palladium membrane.

The DSC was calibrated for temperature and energy changes using indium and zinc as standards, and the system was further checked by comparing the measured heat of palladium hydride formation with values reported in the literature. This internal standard proved invaluable in clarifying and eliminating artifacts which can alter energy change measurements (*10*). The influence of operating parameters such as the temperature of the DSC heat sink (block), the composition of the purge gas, and the catalyst sample size was also examined. In earlier studies, heats of adsorption of hydrogen were measured in a flowing mixture of H_2 and Ar. Because chemisorption and absorption of hydrogen occur only on the sample side, a difference in gas composition between the sample and reference sides is created during the adsorption process. Since H_2 has a much higher thermal conductivity than Ar, the heat transfer from the sample side to the heat sink decreases relative to the reference side due to the gas composition difference, and the apparent energy change is overestimated. This problem can be circumvented by keeping the heat sink at a temperature only slightly below the adsorption temperature and by using He as the carrier gas for H_2 as they have similar thermal conductivities. Details of the modification and calibration of the DSC are provided elsewhere (*10*).

Between 30 and 100 mg of each catalyst was placed in the sample holder and an equal amount of pure support was placed in the reference holder to balance energy changes due to physical adsorption of the gas on the support. When unsupported Pd was examined, a piece of stainless steel or aluminum was placed in the reference holder. The same pretreatment procedures used for the chemisorption measurements were repeated before each heat of adsorption measurement; however, all reductions were carried out in a gas mixture of 8 cm^3 min^{-1} H_2 and 32 cm^3 min^{-1} Ar, and removal of adsorbed H_2 from the catalyst was accomplished by purging the sample with 40 cm^3 min^{-1} Ar for 1 h either at the reduction temperature or at 20–50 K below the reduction temperature if the sample was reduced at 673 K or higher. Purging for more then 1 h did not affect the energy change measured for H_2 chemisorption, which indicated that complete removal of H_2 with no subsequent O_2 contamination was achieved after 1 h. After the pretreatment, the sample was cooled to 300 K, the purge gas was switched from Ar to 40 cm^3 min^{-1} He, a step change to a constant H_2 pressure in the carrier gas (usually 150 Torr) was made via a switching valve, the energy change due to both adsorption and absorption of H_2 was recorded as a function of time and it was then integrated to give the total energy change. After the initial H_2 exposure, the sample was purged with pure He at 300 K for 1 h to decompose the bulk palladium hydride and leave only chemisorbed hydro-

gen (*15*), then H_2 was reintroduced to reform the bulk hydride and the energy change for this process was also measured.

RESULTS

Chemisorption

Uptakes of irreversibly adsorbed hydrogen were determined from the difference between the dual isotherms obtained by the method of Benson *et al.* (*15*), as shown in Fig. 1, and chemisorption uptakes of O_2 were determined by extrapolating the adsorption isotherms to zero pressure to subtract oxygen physisorbed on the support. The H_2 isotherms showed different characteristics (Fig. 1b and c) as a consequence of apparent changes in bulk hydride formation in these samples, as discussed later. Chemisorption of hydrogen on the unsupported Pd sample was measured at pressures below 10 Torr to eliminate formation of the β-hydride phase (H/Pd = 0.6), the presence of which would make measurements of small chemisorption values very difficult. Since monolayer coverage of hydrogen on Pd is achieved at very low pressures, chemisorption uptakes determined at 6 or 150 Torr should be similar. The final uptakes of H_2 and O_2, obtained after a number of pretreatment cycles, are listed in Table 2. The dispersion, D (or fraction exposed), was calculated by assuming a chemisorption stoichiometry of $H_{ad}/Pd_s = 1$ where Pd_s is a surface Pd atom, and the bulk hydride ratio was defined as H_{ab}/Pd_b, where H_{ab} represents the uptake based on reversible H_2 uptakes at 150 Torr, and $Pd_b = Pd_{total} - Pd_s$.

Gas uptakes were usually stable after one pretreatment, and exposure to air at room temperature had no significant effect on the uptakes. Heating in O_2 at 573 K for certain samples also did not change the uptakes. However, gas uptakes frequently decreased after samples were exposed to CO at 300 K, and the effect of CO was particularly noticeable for the most highly dispersed Pd catalysts or the samples reduced

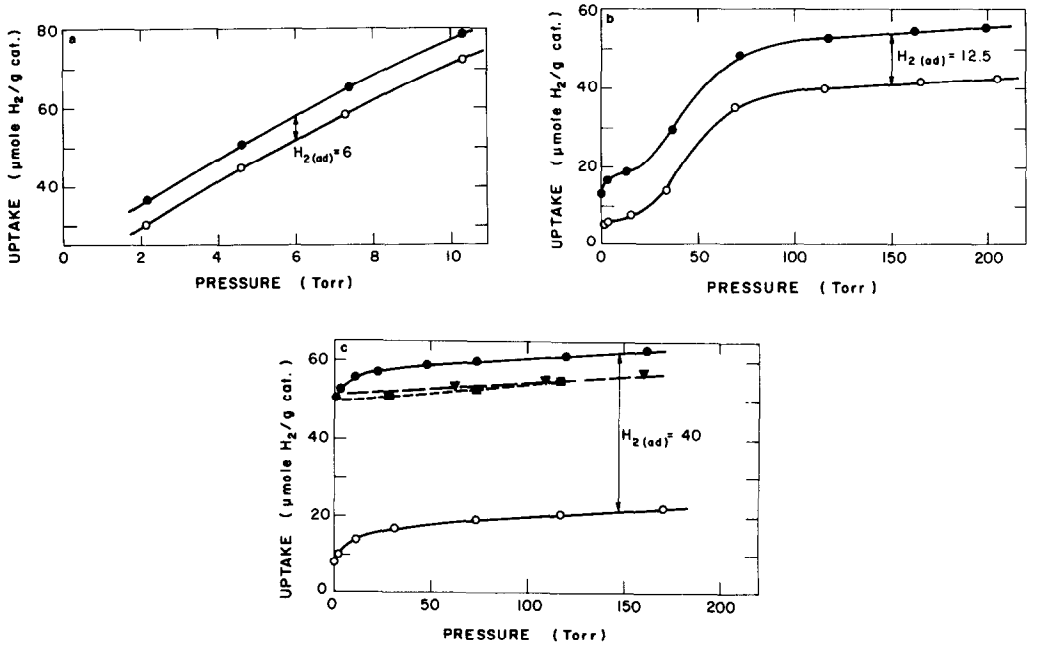

FIG. 1. Hydrogen and oxygen uptakes on Pd samples: (a) Unsupported Pd powder (Sample I), (b) 1.95% Pd/SiO_2–Al_2O_3 (T_r = 673 K), (c) 1.23% Pd/SiO_2 (sample I). H_2 uptakes at 300 K (●,○); H_2 uptakes at 373 K (▼); O_2 uptakes at 300 K (■). Solid symbols: total uptakes; open symbols: reversible uptakes.

at 448 K. The effect of CO on the most highly dispersed Pd samples is attributed to a change in dispersion as discussed elsewhere (*11*). Because of the possibility that a reduction in H_2 at 448 K for 1 h is not sufficient to remove all the strongly bound CO from the Pd surface, after each exposure to CO these samples were treated in a flowing O_2/He mixture at 573 K for 30 min then given a routine reduction. To avoid this complication, H_2 and O_2 uptakes were measured on samples that had not been exposed to CO, except for the three samples indicated in Table 2.

TABLE 2

Gas Uptakes of Absorbed Hydrogen and Chemisorbed Hydrogen and Oxygen

Catalyst (sample)	Pretreatment		Gas uptake (μmole/g cat)			Fraction exposed (H_{ad}/Pd_{total})	Bulk hydride ratio (H_{ab}/Pd_b)
	T_i (K)	T_r (K)	Chemisorption		Absorption		
			O_2	H_2	H_2		
1.71% Pd/SiO_2							
(I-a)	533	673	—	9	36	0.11	0.50
(I-b)	533	673	7.5	8.5	35	0.11	0.49
0.48% Pd/SiO_2							
(I-a)	300	573	—	11	11	0.49	0.95
(I-b)	300	573	12.8	10	11.5	0.44	0.92
2.10% Pd/SiO_2							
(I)	300	573	74.5	67	33	0.68	1.04
(II)	533	673	68	65.5	30.5	0.66	0.92
1.23% Pd/SiO_2							
(I)	300	573	49.5	40	22	0.69	1.24
(II)	533	673	49	36.5	20	0.63	0.94
0.39% Pd/SiO_2							
(I-a)	300	573	—	8	6.5	0.44	0.63
(I-b)	300	573	13.5	9	7.5	0.49	0.80
1.95% Pd/SiO_2–Al_2O_3							
(I-a)	448	448	—	35.5	39	0.39	0.69
(I-b)	448	448	24	32.5	41	0.35	0.69
(II)	448	673	29.5	26.5	30.5	0.29	0.47
(III)	533	673	19	18	33	0.21	0.45
(IV)	673	673	18.5	16	37.5	0.17	0.50
1.16% Pd/SiO_2–Al_2O_3							
(I-a)	300	573	—	30	16	0.55	0.65
(I-b)	300	573	27.5	32	16.5	0.59	0.73
0.98% Pd/SiO_2–Al_2O_3							
(I)	300	573	26.5	28.5	17.5	0.62	0.97
(II)	533	673	21.5	21	19	0.46	0.76
1.80% Pd/Al_2O_3							
(I-a)	533	673[a]	—	39.5	30	0.47	0.67
(I-b)	533	673[a]	19.5	28.5	34.5	0.34	0.62
0.32% Pd/Al_2O_3							
(I-a)	300	573	—	7	5.5	0.47	0.68
(I-b)	300	573	10.5	7.5	5	0.50	0.66
0.36% Pd/Al_2O_3							
(I)	448	448	9.5	10	6.5	0.59	0.94
(II)	300	573	7.5	9.5	6.5	0.56	0.88

TABLE 2—*Continued*

Catalyst (sample)	Pretreatment		Gas uptake (μmole/g cat)			Fraction exposed (H_{ad}/Pd_{total})	Bulk hydride ratio (H_{ab}/Pd_b)
	T_i (K)	T_r (K)	Chemisorption		Absorption		
			O_2	H_2	H_2		
0.54% Pd/Al_2O_3	300	573	20.5	13.5	9.5	0.53	0.80
2.33% Pd/Al_2O_3							
(I)	300	573	28.5	52	34	0.48	0.59
(II)	533	673	33	41	35	0.37	0.51
2.03% Pd/TiO_2							
(LTR-I)	448	448[a]	23	30	51.5	0.31	0.79
(LTR-II)	448	448	19	29.5	52	0.31	0.79
(HTR-I)	448	773	—	1.7	19	—	—
(HTR-II)	448	773	—	1.3	21.8	—	—
1.88% Pd/TiO_2							
LTR-I-a	448	448	14	14	44	0.16	0.59
LTR-1-b	448	448	13	14.5	44.5	0.16	0.60
Pd Powder							
I	300	573	2.5	6[b]	51.5[b]	~0	(0.01)
II	300	573	—	—	3,100	—	0.66

Note. T_i, Temperature at which H_2 was introduced; T_r, reduction temperature.

[a] Samples exposed to CO and treated in 20% O_2 at 573 K.

[b] Uptakes at 6 Torr.

Heats of Adsorption

A typical DSC run is shown in Fig. 2a. Hydrogen chemisorption on Pd proceeded rapidly, and the energy change due to adsorption was typically completed in less than 2 min when samples were exposed to a mixture of 9 cm^3 min^{-1} H_2 and 36 cm^3 min^{-1} He. Bulk hydride formation was also very fast because Pd particles in our samples had a large surface-to-volume ratio. Heats of adsorption on the Pd powder (Fig. 2b) were measured at a much lower H_2 partial pressure (6 Torr) to prevent large energy changes due to the bulk β-hydride phase. Most of the samples were completely reduced after 1 h in the DSC, as indicated by reproducible results following longer reduction periods of the same samples. However, the Pd/TiO_2 (HTR) samples required a longer reduction period before measured heats of adsorption became constant within experimental error, presumably because in the DSC the H_2 had to diffuse through the powder rather than flowing through it as in the adsorption cell, and therefore reduction of TiO_2 to its final state was less efficient in the DSC. The measured energy changes in the DSC, ΔE, the calculated heats of adsorption, Q_{ad} (or $-\Delta H_{ad}$), and the heats of bulk hydride formation, Q_{ab} (or $-\Delta H_{ab}$), are listed in Table 3. The last two sets of data are also plotted versus the average Pd particle size in Figs. 3 and 4 using the relationship d (nm) = $1.13/D$ (*16*). Measurements in the DSC were repeated at least once for each sample and the listed values represent an average of these runs. It should be pointed out that the data points in Figs. 3 and 4 reflect uncertainties in measurements of gas uptake, energy change, and Pd weight loading.

DISCUSSION

Chemisorption

Hydrogen chemisorption has frequently been used to measure the dispersion (frac-

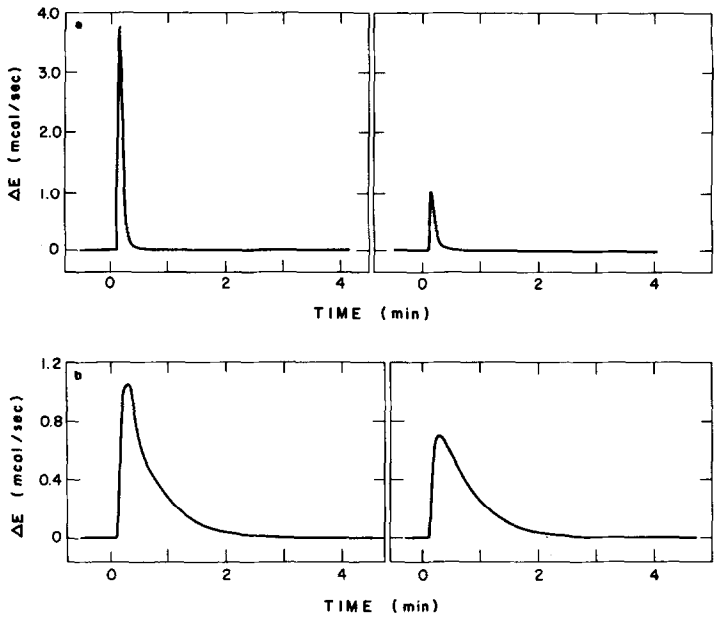

FIG. 2. Energy changes, ΔE, measured at 300 K during hydrogen adsorption and absorption on Pd catalysts (left side) and absorption only (right side). (a) 0.98% Pd/SiO_2–Al_2O_3 (sample II, 0.0340 g), (b) Pd powder (sample I, 0.1064 g).

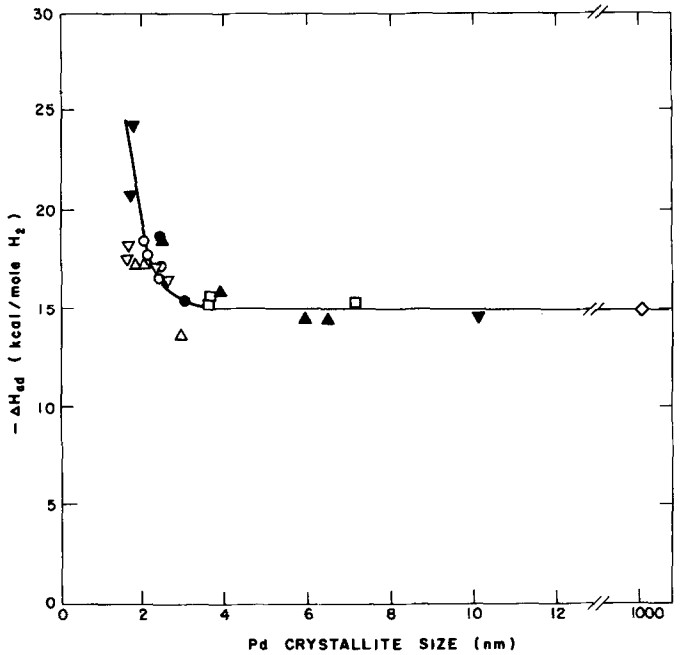

FIG. 3. Heats of adsorption of hydrogen on Pd catalysts ($Q_{ad} = -\Delta H_{ad}$): Pd/SiO_2 (▼,▽), Pd/SiO_2–Al_2O_3 (▲,△), Pd/Al_2O_3 (●,○), Pd/TiO_2 (□), Pd powder (◇). Solid symbols: samples reduced at 673 K; open symbols: samples reduced at 573 or 448 K.

TABLE 3

Heats of Adsorption of Hydrogen on Palladium Catalysts, Q_{ad}, and Heats of Formation of Palladium Hydride, Q_{ab}

Catalyst (sample)	Reduction temperature (K)	d (nm)[a]	Energy change[b] (mcal/g cat)		Q_{ad} (kcal mole^{-1} H_2)	Q_{ab} (kcal mole^{-1} H_2)
			ΔE_{ad}	ΔE_{ab}		
1.71% Pd/SiO_2						
(I-a)	673	10.1	130	278	14.5 ± 0.8	7.7 ± 0.3
0.48% Pd/SiO_2						
(I-a)	573	2.3	188	104	17.0 ± 0.7	9.5 ± 0.3
2.10% Pd/SiO_2						
(I)	573	1.7	1204	419	18.0 ± 0.5	12.7 ± 1.8
(II)	673	1.7	1352	496	20.7 ± 1.6	16.3 ± 0.9
1.23% Pd/SiO_2						
(I)	573	1.6	698	256	17.4 ± 0.6	11.6 ± 0.4
(II)	673	1.7	883	284	24.2 ± 0.2	14.2 ± 2.0
0.39% Pd/SiO_2						
(I-a)	573	2.5	130	64	16.3 ± 0.1	9.9 ± 0.3
1.95% Pd/SiO_2–Al_2O_3						
(I-a)	448	2.9	490	409	13.7 ± 0.5	10.1 ± 0.3
(II)	673	3.9	422	285	15.9 ± 0.3	9.4 ± 0.2
(III)	673	5.9	259	259	14.8 ± 2.0	7.8 ± 1.0
(IV)	673	6.5	237	307	14.4 ± 0.5	8.4 ± 0.1
1.16% Pd/SiO_2–Al_2O_3						
(I-a)	573	2.1	516	189	17.2 ± 0.1	11.8 ± 0.1
0.98% Pd/SiO_2–Al_2O_3						
(I)	573	1.8	500	182	17.5 ± 0.1	10.7 ± 0.1
(II)	673	2.5	390	198	18.6 ± 1.8	10.5 ± 0.5
1.80% Pd/Al_2O_3						
(I-a)	673	2.4	730	316	18.5 ± 0.2	10.5 ± 0.3
0.32% Pd/Al_2O_3						
(I-a)	573	2.4	119	51	17.1 ± 1.2	9.4 ± 0.5
0.36% Pd/Al_2O_3						
(II)	573	2.0	175	64	18.4 ± 1.7	9.8 ± 0.7
0.54% Pd/Al_2O_3	573	2.1	238	93	17.6 ± 0.5	9.8 ± 0.4
2.33% Pd/Al_2O_3						
(I)	573	2.4	851	392	16.4 ± 0.2	11.5 ± 0.1
(II)	673	3.0	631	335	15.4 ± 0.1	9.6 ± 0.1
2.03% Pd/TiO_2						
(LTR-I)	448	3.6	452	470	15.1 ± 0.4	9.0 ± 0.3
(LTR-II)	448	3.7	457	500	15.5 ± 1.1	9.6 ± 0.1
(HTR-I)	773	—	23	159	13.3 ± 0.8	8.4 ± 0.4
(HTR-II)	773	—	25	177	19.2 ± 1.2	8.1 ± 0.2
1.88% Pd/TiO_2						
(LTR-I-a)	448	7.1	214	385	15.3 ± 0.2	8.8 ± 0.3
Pd powder						
(I)	573	1000	89[c]	300[c]	14.9 ± 0.3	5.8 ± 0.1
(I)			—	26,054	—	8.4
(II)	573	1000	—	28,063	—	9.1 ± 0.1

[a] Based on H_2 chemisorption uptakes.
[b] Average value based on 2 to 4 runs.
[c] Measurements made at 6 Torr of H_2.

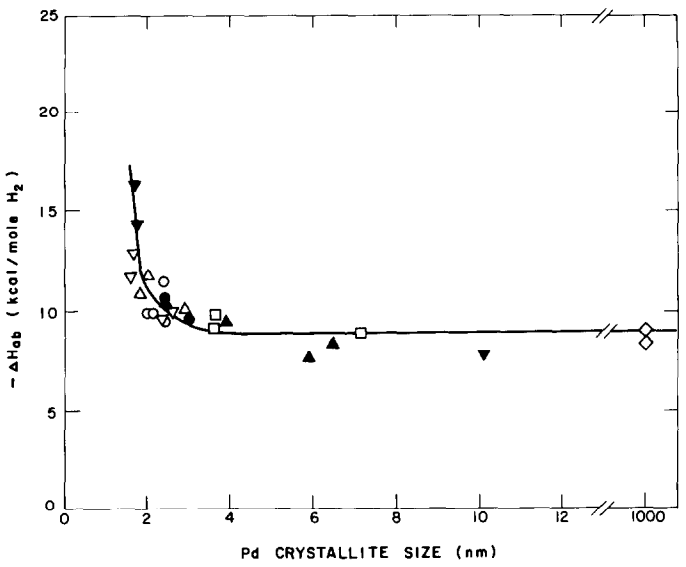

FIG. 4. Heats of formation of β-phase Pd hydride at 300 K ($Q_{ab} = -\Delta H_{ab}$). Symbols: same as for Fig. 3.

tion exposed) of many Group VIII metals. The measurement for Pd, however, is complicated by the formation of bulk Pd hydride in the temperature and pressure ranges normally used for chemisorption measurements. This problem can be resolved by conducting measurements under conditions such that bulk hydride formation is negligible (*17, 18*) or by using the dual-isotherm method of Benson *et al.* (*15*). Because the DSC was operated at 300 K and a H_2 partial pressure of 150 Torr, the dual-isotherm method was used for chemisorption measurements in this study. The results of this method were shown to be in good agreement with results of other techniques such as the O_2–H_2 titration and chemisorption of O_2 and CO when applied to a sample with a relative low dispersion of 0.2 (*15*).

The data in Table 2 indicate that chemisorption uptakes of O_2 tended to be similar to or somewhat lower than those of H_2 on samples with lower dispersions while they frequently were higher than H_2 uptakes on samples with the highest dispersion. The first variation can be due to a chemisorption stoichiometry less than unity for oxygen adsorbed on surfaces dominated by close-packed Pd planes (*19*), which is expected for large particles. As the particle size decreases, the stoichiometry of oxygen adsorption might be expected to increase as the packing of surface Pd atoms become more open; however, the chemisorption stoichiometry of oxygen is unlikely to exceed that of hydrogen on Pd, and the higher O_2 uptakes on highly dispersed Pd, compared to H_2, are attributed to an underestimated H_2 uptake provided by the dual-isotherm method, as suggested by the following evidence. When Pd is exposed to H_2, the Pd surface is first saturated with chemisorbed hydrogen at very low pressure, and with increasing H_2 pressure the α-phase Pd hydride is formed. At 300 K the α-phase saturates at a H_{ab}/Pd_b ratio of 0.015 near 15 Torr (*20*), and if additional H_2 is added, the α-phase transforms into the β-phase until completion of this process at a H_{ab}/Pd_b ratio near 0.55–0.60 (*21*). Although transformation to the β-phase is frequently not sharp with well-dispersed Pd, Fig. 1b clearly shows the onset of this change at pressure above 15 Torr, and a bulk hydride ratio of 0.52 is calculated from the back-

sorption isotherm at 150 Torr. However, the normal characteristics of β-phase formation become virtually indiscernible in the isotherms measured for one of the most highly dispersed samples (Fig. 1c), and the hydride ratio calculated from these isotherms would be equal to 1.24 (Table 2) if all of the reversible H_2 uptake is associated only with bulk hydride formation. Although hydride ratios near unity have been reported, these require extreme conditions or special preparation methods (*21*). Therefore, the high apparent hydride ratios are likely due to an overestimated amount of absorbed hydrogen by the backsorption isotherm. Indeed, if this isotherm measures only uptake due to bulk hydride formation, the isotherm should intercept the ordinate at the origin (*20*), but the backsorption isotherms in Figs. 1b and c both indicate finite uptakes at very low pressure. Apparently, some weakly adsorbed hydrogen was removed by the evacuation that decomposed the bulk hydride, and Fig. 1c indicates that at 300 K about 15% of the total adsorbed hydrogen on Pd can be removed by the evacuation, as the adsorption capacity for both O_2 at 300 K and H_2 at 373 K, where bulk hydride formation is negligible, was about 50 μmole g^{-1} on that sample.

Since the same sorption–backsorption method was used in both chemisorption and DSC measurements, the heats of adsorption obtained in this study were not affected by this complication, and they represent integral values for the irreversibly adsorbed hydrogen. However, the behavior does imply that dispersions estimated from the H_2 uptakes in Table 2 are somewhat underestimated and that the integral heats of adsorption correspond to near monolayer, rather than complete, coverage of adsorbed hydrogen. A precise determination of the uptake corresponding to monolayer coverage of hydrogen may be difficult because the Pd–H bonding strength decreases as the coverage approaches unity, and a distinction between weakly adsorbed hydrogen and absorbed hydrogen becomes difficult. The situation is further complicated by the possibility of adsorption on subsurface sites (*22*), which has been suggested as the precursor of absorbed hydrogen (*23*) and could account for a major portion of the uptake measured in the range from near 0 to 15 Torr, as shown in Figs. 1b and c.

Heats of Adsorption

Table 4 lists Q_{ad} values for hydrogen on Pd reported in the literature, and most of the data correspond to initial heats of adsorption, which normally range from 21 to 26 kcal $mole^{-1}$ and are not too sensitive to the type of Pd surface. The values of Q_{ad} remain fairly constant up to medium coverages and then decrease at higher coverages. Integral heats of adsorption have been estimated from these results when variations of Q_{ad} with surface coverage were given in the original papers, and they are also listed in Table 4. These Q_{ad} values were often reported only for limited ranges of hydrogen coverages, which in some cases were determined indirectly by measuring changes in the work function; therefore, the estimated integral heats of adsorption from these results clearly contains some uncertainty. Regardless, they should provide reasonable values and the results from this study compare well with these estimated values. For example, the larger Pd crystallites gave a constant Q_{ad} value near 15 kcal $mole^{-1}$, independent of the support as shown in Fig. 3, compared to 20 kcal $mole^{-1}$ estimated for the Pd(111) plane. This former value is even closer to that of 14 kcal $mole^{-1}$ estimated for a Pd/MgO sample. Since one major objective was to investigate the influence of Pd crystallite size and support on heats of adsorption, effects of these two parameters are discussed separately.

Crystallite Size Effect

As shown in Fig. 3, the Q_{ad} for hydrogen remains essentially constant at 15 $\pm$ 1 kcal $mole^{-1}$ as the crystallite size decreases from 1000 to 3 nm, but it increases sharply as the size drops below 3 nm, with the high-

TABLE 4

Initial Heats of Adsorption and Estimated Integral Heats of Adsorption of H_2 on Pd from Previous Studies

Surface	$Q_{initial}$ (kcal mole^{-1} H_2)	$Q_{integral}$ (kcal mole^{-1} H_2)	Technique	Ref.
Pd(111)	21	20.2[b]	Isosteric	(*24*)
Pd(111)	23.7[a]	—	TPD	(*24*)
step/Pd(111)	23.8	—	Isosteric	(*24*)
Pd(100)	24.5	23.5[b]	Isosteric	(*25*)
Pd(100)	22[a]	—	TPD	(*25*)
Pd(110)	24.4	22.5[b]	Isosteric	(*24*)
Pd(110)	23[a]	—	TPD	(*24*)
Pd filament	22, 25, 35[a]	—	TPD	(*26*)
Pd/MgO	26.3 (d = 2.5 nm)	17.7	Calorimetric	(*27*)
	19 (d = 7.5 nm)	13.5		
	24.6 (d = 12.4 nm)	13.9		
Pd film	26		Calorimetric	(*1*)
Pd/C	25		Isosteric	(*28*)
Pd/C	21[a]		TPD	(*29*)

[a] Thermal desorption results.

[b] Maximum values based on work function change.

est value of 24 kcal mole^{-1} being obtained on the most highly dispersed samples. A similar size effect has previously been reported for H_2 heats of adsorption on Pd/MgO samples (*27*).

In a number of cases, crystallite size has been shown to be an important parameter in catalysis. It has been suggested that these effects can be a consequence of a variation in the number and arrangement of nearest neighbors of surface atoms as crystallite size changes (*9*). On the other hand, size effects can be due to changes in the electronic structure as a cluster of metal atoms grows into larger crystallites which finally develop the electronic band structure of bulk metal (*8*). The effect of the geometric factor on Q_{ad} can be examined by comparing the values measured on different single-crystal planes. Data in Table 4 suggest that Q_{ad} might increase slightly as Pd crystallite size decreases because the arrangement of surface atoms becomes more open and the number of step sites is also expected to increase as size decreases. However, it is interesting to note that the variation of Q_{ad} over the size range studied is larger than that which might be attributable to changes in surface geometry alone. This implies that electronic properties of small crystallites also contribute to the larger heats of adsorption measured on the highly dispersed samples.

Electronic properties of small Pd crystallites or clusters have been described by both model calculations (*30–32*) and characterized by different experimental methods (*33, 34*). Some of these calculations have indicated that a crystallite must contain more than 100 atoms to develop electronic properties comparable to those of bulk metal (*30*). This prediction has been supported by XPS and UPS data, which indicated that the electronic behavior of small Pd crystallites converged to that of bulk Pd metal as the crystallite size increased to about 2–3 nm (*33, 34*); therefore, our results are very consistent with these XPS and UPS data. Using X-ray absorption spectroscopy, Mason has shown that smaller Pd clusters have a large number of *d*-orbital vacancies (*35*), and Messmer *et al.* have concluded from model calculations that small metal clusters show a

slight depletion of electron charge on surface atoms (*31*). Both groups suggested that a stronger interaction between small metal clusters and adsorbates is expected. Different approaches in these calculations have been used to investigate the interactions between hydrogen and transition metals. Most of these calculations were focused on the variation of the H–metal bonding strength across the periodic table (*36–40*); however, three studies investigated interactions between hydrogen and Pd clusters (*41–43*), and in one of them bonding between hydrogen and a Pd_4 cluster was found to be much stronger than the bonding of hydrogen to a Pd(111) plane (*43*). A similar size effect on Q_{ad} for CO and oxygen on Pd has also been observed in our studies (*11, 12*).

Small Pd crystallites may possess special catalytic properties which can be related to their stronger interaction with adsorbates. Dissociation of CO has not been reported during thermal desorption of CO from different Pd single-crystal planes (*44*); however, Ichikawa *et al.* have found that small Pd crystallites appear to be able to dissociate CO readily at 373 K during thermal desorption runs (*45*). In another example, Takasu *et al.* have reported a increase of 9.5 kcal $mole^{-1}$ in the activation energy for the H_2–D_2 exchange reaction over Pd/mica catalysts as the Pd crystallite size decreased from 2.4 to 1 nm (*46*). They proposed that this was a consequence of an increase in the activation energy of dissociative adsorption; however, hydrogen adsorption on Pd is rapid, regardless of crystallite size as shown by the rapid formation and decomposition of Pd hydride at 300 K (*15*). Based on our results, a more likely explanation is that desorption is the slow step in this reaction and an increase in Q_{ad} would increase the apparent activation energy, as shown by a simple Langmuir–Hinshelwood model (*47*). Regardless of the ultimate explanations, examples exist of catalytic behavior which changes with crystallite size and may correlate with changes in Q_{ad}.

Support Effect

Since the heat of adsorption changes with Pd crystallite size, support effects on Q_{ad} must be examined at comparable dispersions. As shown in Fig. 3, on all the samples studied, the measured Q_{ad} values basically follow a single trend over the size range from 1000 to 1.6 nm, and no support effect is obvious. The 2.03% Pd/TiO_2 (HTR) samples are not plotted in Fig. 3 because the suppression of chemisorption after (HTR) at 773 K prevents an accurate estimation of Pd crystallite size for these samples; however, since TiO_2-supported Pd begins to show a tendency to sinter at reduction temperatures above 773 K (*48*), it is reasonable to assume that the 2.03% Pd/TiO_2 (HTR) samples have a dispersion comparable to or less than that measured for the low-temperature reduction (LTR) samples. Therefore, the results in Table 3 indicate that despite the sharp decrease in hydrogen chemisorption on the Pd/TiO_2 (HTR) samples, the H_2 heat of adsorption measured on these samples is not significantly different from the other catalysts, within experimental error. Based on XPS data, charge transfer between metal and TiO_2 after HTR has been suggested as the cause for the suppression in chemisorption (*49, 50*). However, interpretations of XPS data are complicated by size-dependent final state effects, and in one case, no evidence of charge transfer was found if such size effects were taken into account (*51*). The explanation invoking a blockage of chemisorption sites by migrating TiO_x species onto the Pd surface does not require a weakened adsorbate–metal interaction and, hence, is supported by our results. Electronic interactions between Pd and conventional supports such as Al_2O_3, SiO_2–Al_2O_3, and zeolites have been proposed based on XPS results and IR data of adsorbed CO (*52, 53*); however, since IR spectra of adsorbed CO can strongly reflect the geometry of the adsorption sites, as mentioned by Shustorovich (*54*), and be-

cause the interpretation of XPS measurements can be complicated, these IR and XPS results do not constitute unambiguous evidence for metal–support interactions. Consequently, for the crystallite size range examined in this study, we conclude no significant Pd–support effect is obvious, and these results suggest that the electronic properties of surface Pd atoms are not markedly affected by the oxide support although metal–support interactions are expected to be more likely to occur when metal clusters containing a small number of atoms are present.

Heat of Absorption

The formation of a stable bulk hydride under mild conditions is a distinctive property of Pd as compared to other group VIII metals. Both model calculations and experimental data have suggested a great similarity between H–Pd interactions in bulk hydride and those between Pd and chemisorbed hydrogen (*41, 55, 56*). Although the heat of bulk hydride formation, Q_{ab}, is much lower than that of adsorption, the Pd–H bond strengths in the two systems are still comparable. As shown in Fig. 4, Q_{ab} changes with Pd crystallite size in a trend almost identical to that observed for Q_{ad}; however, it should be emphasized that the measured Q_{ab} value may not represent the true Q_{ab} value for the more highly dispersed samples because of the removal of weakly adsorbed hydrogen during evacuation, as mentioned in the discussion of chemisorption. Because weakly adsorbed hydrogen contributes to a larger fraction of the reversible uptakes measured on highly dispersed samples, most of the increase in Q_{ab} may be due to a larger contribution from the weakly adsorbed hydrogen. However, a model calculation has suggested a stronger bonding between absorbed hydrogen and Pd should occur in the region near the surface (*57*), which implies that Q_{ab} should increase as the Pd crystallite size decreases and the remaining bulk Pd atoms become adjacent to the surface atoms. This conclusion is further supported by a cluster calculation which has shown a larger than normal H–Pd bonding for a hydrogen atom inside a Pd_4 cluster (*43*). Therefore, size effects may also contribute to some of the increase in the Q_{ab} measured for the highly dispersed samples. For samples with a low surface-to-volume ratio (low dispersion), the contribution from weakly adsorbed hydrogen is negligible and the Q_{ab} values measured for these samples were 8.7 ± 1.0 kcal mole^{-1}, which is close to values ($9.3 + 0.3$ kcal mole^{-1}) reported for bulk Pd in the literature (*58–60*). Most backsorption isotherms were carried out at a H_2 partial pressure of 150 Torr, and the Q_{ab} measured corresponds to formation of the β-phase hydride; however, one measurement for the Pd powder was made at 6 Torr H_2 pressure, and this Q_{ab} of 5.8 kcal mole^{-1} corresponds to formation of the α-phase and is also in good agreement with a value of 5.6 kcal mole^{-1} reported in the literature (*61*).

Bulk hydride formation also provides a test for models proposed to explain the suppression of chemisorption on Pd/TiO_2 (HTR) samples. If this decrease in chemisorption is due to an electronic interaction between Pd crystallites and TiO_2 at the metal–support interface, all the atoms in the Pd crystallites are likely to be affected. Based on this interpretation a suppression of bulk hydride formation comparable to that of chemisorption might be expected; however, data for the 2.03% Pd/TiO_2 samples indicated a much more drastic reduction in hydrogen chemisorption than in bulk hydride formation as the reduction temperature was increased from 448 to 773 K (Table 2). On the other hand, these results are consistent with the explanation that chemisorption suppression is primarily due to blockage of the Pd surface by TiO_x species because bulk hydride formation would not be affected unless the surface of a Pd crystallite was completely blocked or encapsulated so that no H_2 adsorption at all could occur. This interpretation is further supported by the similar Q_{ab} values measured

for the 2.03% Pd/TiO_2 HTR and LTR samples.

SUMMARY

Integral heats of adsorption of hydrogen have been measured calorimetrically on a family of Pd catalysts, and they appear to be insensitive to the support used. Although hydrogen chemisorption on Pd/TiO_2 samples decreases sharply after HTR, hydrogen heats of adsorption on these samples are not significantly different from those on other typical catalysts, within experimental error. Therefore, these results support the explanation that suppressed chemisorption on Pd/TiO_2 (HTR) is due to a blockage of Pd surface sites by migrating TiO_x species. In a number of cases, supports have been reported to affect the catalytic properties of Pd, and the results of this study suggest that if they do, it is through a mechanism which does not require a change in the heat of adsorption. However, the heat of adsorption of hydrogen increases sharply as the Pd crystallite size drops below 3 nm, and such a change may result in the changes in catalytic behavior reported for some reactions. Similar to the Q_{ad}, the heat of hydride formation is unaffected by the support and increases as Pd crystallite size decreases; however, this increase may be partially due to a contribution from weakly adsorbed hydrogen which is removed during hydride decomposition and readsorbed during its formation.

ACKNOWLEDGMENT

This study was supported by the U.S. DOE, Division of Basic Energy Sciences, under Grant DD-FG02-84ER13276.

REFERENCES

1. Beeck, O., *Discuss. Faraday Soc.* **8,** 118 (1950).
2. Tauster, S. J., Fung, S. C., and Garten, R. L., *J. Amer. Chem. Soc.* **100,** 170 (1978).
3. Tauster, S. J., and Fung, S. C., *J. Catal.* **55,** 29 (1978).
4. Tauster, S. J., Fung, S. C., Baker, R. T. K., and Horsley, J. A., *Science* **211,** 1121 (1981).
5. (a) Meriaudeau, P., Dutel, J., Dufaux, M., and Naccache, C., *in* "Studies in Surface Science and Catalysis" (B. Imelik *et al.*, Eds.), Vol. 11, p. 95. Elsevier, New York, 1982. (b) Meriaudeau, P., Ellestad, O. H., Dufaux, M., and Naccache, C., *J. Catal.* **75,** 243 (1982).
6. Santos, J., Phillips, J., and Dumesic, J. A., *J. Catal.* **81,** 147 (1983).
7. Boudart, M., *in* "Proceedings, Sixth International Congress on Catalysis, London, 1976" (G. C. Bond *et al.*, Eds.), Vol. 1, p. 1. Chem. Soc., London, 1977.
8. Baetzold, R. C., and Hamilton, J. F., *Prog. Solid State Chem.* **15,** 1 (1983).
9. van Hardeveld, R., and Hartog, F., *in* "Advances in Catalysis" (D. D. Eley, P. W. Selwood, P. B. Weisz, Eds.), Vol. 22, p. 75. Academic Press, Orlando, FL, 1972.
10. Vannice, M. A., Sen, B., and Chou, P., submitted for publication.
11. Chou, P., and Vannice, M. A., *J. Catal.* **104,** 17–30 (1987).
12. Chou, P., and Vannice, M. A., *Rev. Sci. Instrum.*, in press.
13. Boitiaux, J. P., Cosyns, J., and Vasudevan, S., *Sci. Bases Prep. Heterog. Cat.*, A10.1 (1982).
14. Palmer, M. B., and Vannice, M. A., *J. Chem. Technol. Biotechnol.* **30,** 205 (1980).
15. Benson, J. E., Hwang, H. S., and Boudart, M., *J. Catal.* **30,** 146 (1973).
16. Wang, S. Y., Moon, S. H., and Vannice, M. A., *J. Catal.* **71,** 167 (1981).
17. Aben, P. C., *J. Catal.* **10,** 224 (1968).
18. Sermon, P. A., *J. Catal.* **24,** 460 (1972).
19. Conrad, H., Ertl, G., Küppers, J., and Latta, E. E., *Surf. Sci.* **65,** 245 (1977).
20. Wicke, E., and Nernst, G. H., *Ber. Bunsenges. Phys. Chem.* **68,** 224 (1964).
21. Mueller, W. M., Blackledge, J. P., and Libowitz, G. G., "Metal Hydrides." Academic Press, New York, 1968.
22. Cattania, M. G., Penka, V., Behm, R. J., Christmann, K., and Ertl, G., *Surf. Sci.* **126,** 382 (1983).
23. Lynch, J. F., and Flanagan, T. B., *J. Phys. Chem.* **77,** 2628 (1973).
24. Conrad, H., Ertl, G., and Latta, E. E., *Surf. Sci.* **41,** 435 (1974).
25. Behm, R. J., Christmann, K., and Ertl, G., *Surf. Sci.* **99,** 320 (1980).
26. Aldag, A. W., and Schmidt, L. D., *J. Catal.* **22,** 260 (1971).
27. Zakumbaeva, G. D., Zakarina, N. A., Naidin, V. A., Dostiyarov, A. M., Toktabaeya, N. F., and Litvyakova, É. N., *Kinet. Catal.* **24,** 379 (1983).
28. Gentsch, H., Guillen, N., and Köpp, M., *Z. Phys. Chem. N.F.* **82,** 49 (1972).
29. Konvalinka, J. A., and Scholten, J. J. F., *J. Catal.* **48,** 374 (1977).

30. Baetzold, R. C., Mason, M. G., and Hamilton, J. F., *J. Chem. Phys.* **72,** 366 (1980).
31. Messmer, R. P., Kundson, S. K., Johnson, K. H., Diamond, J. B., and Yang, C. Y., *Phys. Rev. B* **13,** 1396 (1976).
32. Tanabe, T., Adachi, H., and Imoto, S., *Japan. J. Appl. Phys.* **16,** 1097 (1977).
33. Mason, M. G., Gerenser, L. J., and Lee, S.-T., *Phys. Rev. Lett.* **39,** 288 (1977).
34. Takasu, Y., Unwin, R., Tesche, B., Bradshaw, A. M., and Grunze, M., *Surf. Sci.* **77,** 219 (1978).
35. Mason, M. G., *Phys. Rev. B* **27,** 748 (1983).
36. Nordlander, P., Holloway, S., and Nørkov, J. K., *Surf. Sci.* **136,** 59 (1984).
37. Muscat, J. P., *Surf. Sci.* **110,** 389 (1981).
39. Shustorovich, E., Baetzold, R. C., and Muetterties, E. L., *J. Phys. Chem.* **87,** 1100 (1983).
39. Varma, C. M., and Wilson, A. J., *Phys. Rev. B* **22,** 3795 (1980).
40. Doyen, G., and Ertl, G., *J. Chem. Phys.* **68,** 5417 (1978).
41. Messmer, R. P., Salahub, D. R., Johnson, K. H., and Yang, C. Y., *Chem. Phys. Lett.* **51,** 84 (1977).
42. Baetzold, R. C., *Surf. Sci.* **51,** 1 (1975).
43. Miyoshi, E., Sakai, Y., and Mori, S., *Surf. Sci.* **158,** 667 (1985).
44. (a) Ertl, G., and Koch, J., *in* "Proceedings, Fifth International Congress on Catalysis, Palm Beach, 1972" (J. W. Hightower, Ed.), Vol. 2, p. 969. North-Holland, Amsterdam, 1973. (b) Conrad, H., Ertl, G., Koch, J., and Latta, E. E., *Surf. Sci.* **43,** 462 (1974).
45. Ichikawa, S., Poppa, H., and Boudart, M., *ACS Symp. Ser.* **248,** 439 (1983).
46. Takasu, Y., Kasahara, K., and Matsuda, Y., *Bull. Chem. Soc. Japan* **57,** 2313 (1984).
47. Engel, T., and Ertl, G., *Chem. Phys. Solid Surf. Heterog. Catal.* **4,** 195 (1982).
48. Baker, R. T. K., Prestridge, E. G., and McVicker, G. B., *J. Catal.* **89,** 422 (1984).
49. Fung, S. C., *J. Catal.* **76,** 225 (1982).
50. Kao, C. C., Tsai, S. C., Bahl, M. K., and Chung, Y. W., *Surf. Sci.* **95,** 1 (1980).
51. Huizinga, T., and Prins, R., *in* "Metal–Support and Metal–additive Effects in Catalysis" (B. Imelik *et al.*, Eds.), p. 11. Elsevier, New York, 1982.
52. Figueras, F., Gomez, R., and Primet, M., *Adv. Chem. Ser.* **121,** 480 (1973).
53. Antoshin, G. V., Shpiro, E. S., Tkachenko, O. P., Nikishenko, S. B., Ryashontseva, M. A., Avaev, V. I., and Minachev, Kh. M., *in* "Proceedings, Seventh International Congress on Catalysts, Tokyo, 1980," p. 302. Elsevier, Amsterdam/New York.
54. Shustorovich, E., *Surf. Sci. Rep.* **6**(1), 1986.
55. Eastman, D. E., Cashion, J. K., and Switendick, A. C., *Phys. Rev. Lett.* **27,** 35 (1971).
56. Conrad, H., Ertl, G., Küppers, J., and Latta, E. E., *Surf. Sci.* **58,** 578 (1976).
57. Lagos, M., and Schuller, I. K., *Surf. Sci.* **138,** L161 (1984).
58. Nace, D. M., and Aston, J. G., *J. Amer. Chem. Soc.* **79,** 3619 (1957).
59. Picard, C., Kleppa, O. J., and Boureau, G., *J. Chem. Phys.* **69,** 5549 (1978).
60. Kuji, T., Oates, W. A., Bowerman, B. S., and Flanagan, T. B., *J. Phys. F* **13,** 1785 (1983).
61. Lynch, J. F., and Flanagan, T. B., *JCS Faraday Trans. I* **70,** 814 (1974).